Energy Flow in the Super Alfvénic/Sonic Collisional Merging Process of Field-Reversed Configurations*)

Daichi KOBAYASHI, Tomohiko ASAI, Tsutomu TAKAHASHI, Arisa TATSUMI, Naoto SAHARA, Tatsuhiro WATANABE, Daisuke HARASHIMA, Hiroshi GOTA[1)] and Thomas ROCHE[1)]

College of Science and Technology, Nihon University, Tokyo 101-8308, Japan
[1)]*TAE Technologies, Inc., Foothill Ranch, CA 92610, USA*

(Received 16 November 2020 / Accepted 11 February 2021)

Energy flow in the collisional merging process of a field-reversed configuration (FRC) was experimentally evaluated. Collisional merging formation of an FRC was carried out in the FAT-CM (FRC amplification via translation-collisional merging) device. In this experiment, the field-reversed theta-pinch formed FRC-like plasmoids are accelerated due to a magnetic pressure gradient. Then, two plasmoids collide at a relative speed of ~300 km/s, which is faster than typical Alfvén and ion sound speeds (~50 km/s) on the separatrix. The kinetic and internal energy of plasmoids before and after collision are estimated by simultaneous multi-point measurements combining magnetic probes and interferometers. The energy flow in the collisional merging process is compared to an experimental case with single plasmoid translation. This comparison indicates that the kinetic energy of two accelerated plasmoids regenerates back into the internal thermal energy of the FRC after merging. Moreover, density and neutron measurements suggest excitation of shockwaves. These results indicate that shock heating may become a channel for energy regeneration.

Keywords: field-reversed configuration, high beta plasma, FRC merging, shockwave, energy regeneration

DOI: 10.1585/pfr.16.2402050

1. Introduction

A field-reversed configuration (FRC) is an extremely high beta plasmoid that has a solely poloidal flux [1, 2]. The local beta value in most of the FRC volume, except in the vicinity of the separatrix, is above unity.

Collisional merging formation of an FRC has been carried out in the FAT-CM (FRC amplification via translation-collisional merging) device [3]. In this formation technique, two FRC-like magnetized plasmoids, formed using the field-reversed theta-pinch (FRTP) method, are accelerated due to a magnetic pressure gradient. The plasmoids are translated into the confinement region with a quasi-static magnetic field. The plasmoids collide and, at the mid-plane of this region, they merge into a single FRC state. The relative speed of plasmoids before collision exceeds Alfvén and ion sound speeds on the separatrix of plasmoids. The increase of trapped flux and plasma heating have been observed in collisional merging formed FRCs. These phenomena have also been observed in the C-2 series at TAE Technologies, Inc. [4]. The sufficiently trapped flux of FRCs for tangential neutral beam injection (NBI) have been realized in the C-2 series using the collisional merging formation technique. Sustainment of the FRC for over 5 ms with NBI and electric field biasing have been achieved [5]. In experiments on the FIX device, the re-thermalization of a single translated FRC via shockwave excitation in the reflection process, due to a mirror field, has been suggested [6, 7]. Shockwaves will also be excited in the collisional merging process since the plasmoids collide with each other at a relative velocity that is twice the translation velocity in single plasmoid translation experiments [8]. Therefore, shockwaves are considered to play an important role in the increase of trapped flux and plasma heating in the collisional merging process.

In this work, the energy flow in the collisional merging process was experimentally evaluated with simultaneous multi-pointed measurements, which combine magnetic probes and interferometers. The energy flow is discussed by comparison to the single plasmoid translation case.

2. Energy of the FRC

Plasma pressure completely balances with an external magnetic field when approximating a prolate FRC as a columnar shape. Radial pressure balance is constant in most of the prolate FRC volume, except for the axial edges. The magnetic energy inside an FRC can be directly described by $Nk_{\mathrm{B}}T_{\mathrm{total}}$ [9]. The total energy, E_{total}, is defined as the summation of thermal, magnetic, and kinetic energy:

$$E_{\mathrm{total}} = \frac{3}{2}Nk_{\mathrm{B}}T_{\mathrm{total}} + Nk_{\mathrm{B}}T_{\mathrm{total}} + \frac{1}{2}Nm_{\mathrm{i}}v^2. \quad (1)$$

Here, N is the total inventory, k_{B} is Boltzmann's constant, T_{total} is the sum of ion and electron temperature

author's e-mail: csda19001@g.nihon-u.ac.jp

*) This article is based on the presentation at the 29th International Toki Conference on Plasma and Fusion Research (ITC29).

($T_{\text{total}} = T_{\text{i}} + T_{\text{e}}$), m_{i} is the ion mass, and v is the velocity of an FRC. The first, second, and third terms in Eq. 1 indicate thermal, magnetic, and kinetic energy, respectively. The total temperature can be estimated from the external magnetic field intensity, B_{ext}, density, n, and volume-averaged beta, $\langle\beta\rangle$. The total temperature is described as

$$T_{\text{total}} = \frac{{B_{\text{ext}}}^2}{2\mu_0 n k_{\text{B}}}\langle\beta\rangle, \tag{2}$$

and the volume-averaged beta is approximated by

$$\langle\beta\rangle = 1 - \frac{{\chi_{\text{s}}}^2}{2}. \tag{3}$$

Here, χ_{s} is the separatrix radius normalized by the device wall radius. The thermal and magnetic energy can be estimated without a density measurement.

3. Experimental Setup

Figure 1 shows a schematic diagram of the FAT-CM device with diagnostic setup and the axial profile of the external guide magnetic field. The FAT-CM device has two FRTP formation sections at both ends of the confinement section. Formation sections are composed of a transparent quartz tube and conical theta-pinch coils. The conical theta-pinch coils provide a magnetic pressure gradient for acceleration. The confinement section is composed of a stainless-steel chamber and multi-turn coils for a quasi-static confinement magnetic field of ~0.06 T. The metal chamber serves as a flux conserver since the skin time (~5 ms) is much longer than the timescale of the translation and collisional merging processes (several hundreds of microseconds). Deuterium gas is used for plasma generation.

Magnetic probes and flux loops were used to estimate the excluded flux radius [10]. The shape of the FRC separatrix was determined by the axial profile of the excluded flux radius. A set of fourteen magnetic probes and two flux loops were installed on each formation section. Magnetic probes were axially arranged on the quartz tube wall at intervals of 0.11 m. Flux loops were wound on the quartz tube at $z = \pm 2.38$ and ± 3.15 m. Sixteen magnetic probes were also axially arranged on the chamber wall, in the confinement section, at an interval of 0.15 m. The excluded flux radius, $r_{\Delta\phi}$, is calculated by

$$r_{\Delta\phi} = r_{\text{w}}\sqrt{1 - \frac{\phi_{\text{p}} B_{\text{v}}}{\phi_{\text{v}} B_{\text{p}}}}, \tag{4}$$

where r_{w} is the inner radius of the chamber or theta-pinch coils, ϕ is the magnetic flux, and B is the magnetic field density. Subscripts "p" and "v" in Eq. 4 indicate the cases of plasma and vacuum discharge, respectively. The translation velocity of initial FRC-like plasmoids was determined by the time-of-flight method for peaks of the excluded flux radius at each axial point.

Two interferometers were installed on the mid-plane ($z = 0$) of the confinement section and at $z = -0.6$ m. The averaged electron density was estimated by dividing the line-integrated electron density at mid-plane by a plasma diameter of $2r_{\Delta\phi}$. The total particle inventory was estimated by the averaged electron density and the plasma volume calculated using the excluded flux radius.

A neutron detector was installed outside the metal chamber in the confinement section ($z = -0.3$ m). It consists of a plastic scintillator (Eljen Technology, EJ-200) and a photomultiplier tube (PMT) (Hamamatsu Photonics K.K., H6614-70). The scintillator emits when high energy neutrons are injected into the neutron detector. The light emission is detected by a PMT. The scintillator and PMT are in a housing case made of stainless-steel, which shields external light, low energy radiation, and high frequency electromagnetic noise.

4. Experimental Results

4.1 Energy flow in the collisional merging process

Figure 2 shows a typical breakdown of energy in sin-

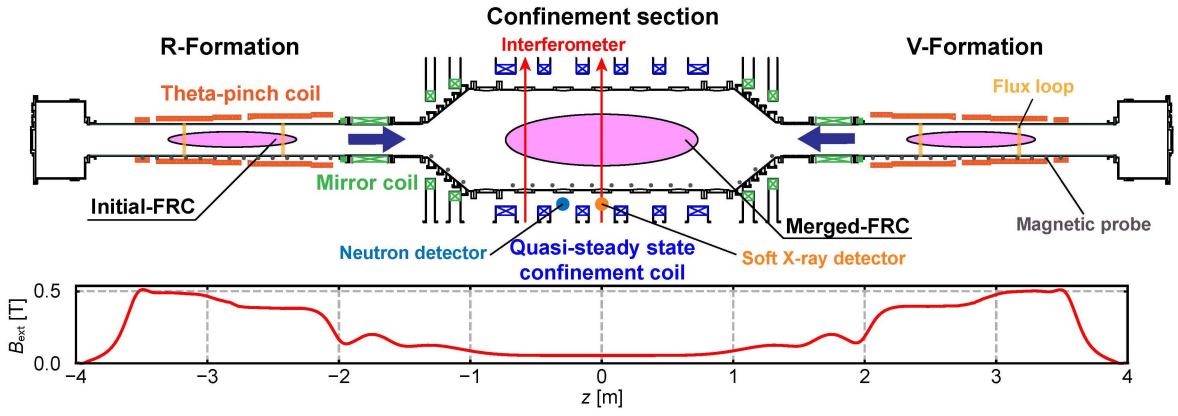

Fig. 1 Schematic diagram of the FAT-CM device with diagnostic setup (top) and the axial profile of the external guide magnetic field (bottom).

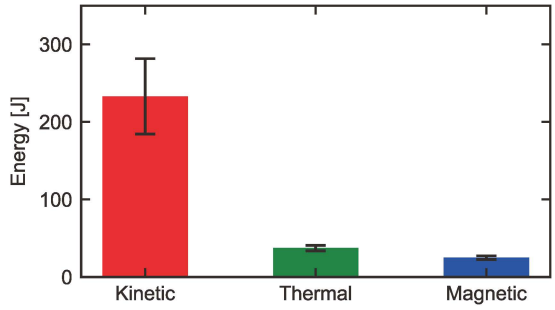

Fig. 2 Energy breakdown of the translated FRC-like plasmoid at mid-plane.

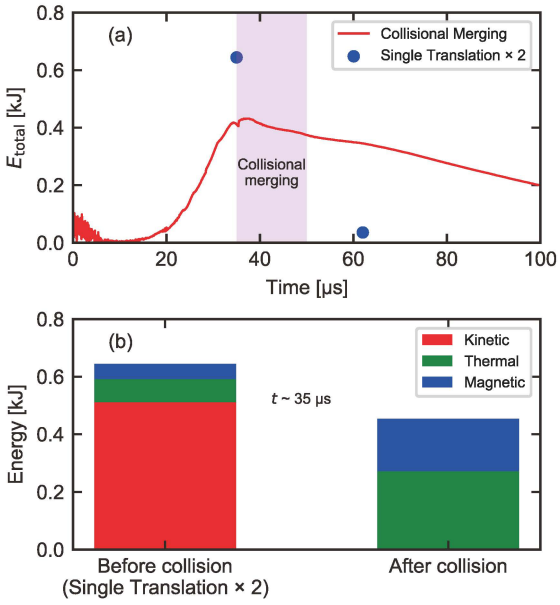

Fig. 3 (a) Time evolution of total energy and (b) breakdown of energy before and after the collision.

gle plasmoid translation when the plasmoid passes through the mid-plane. The typical translation velocity was around 150 km/s, which exceeds the Alfvén speed (~50 km/s) and ion sound speed (~50 km/s), on the separatrix. The kinetic energy is dominant over the thermal and magnetic energy of the translated plasmoid at mid-plane. The kinetic energy would be more dominant in the collisional merging formation process.

Figure 3 shows a comparison of energy time evolution between the single plasmoid translation case and the collisional merging case. The red line in Fig. 3 (a) denotes the total energy of the collisional merging formed FRC. This total energy does not include the kinetic energy since the FRC after merging is almost still in the axial direction. The blue dots in the figure indicate the total energy of the single translated plasmoid at each time. The kinetic energy in single plasmoid translation cases can be obtained only at the time when the plasmoid passes through the measurement point of the interferometer. This total energy is doubled

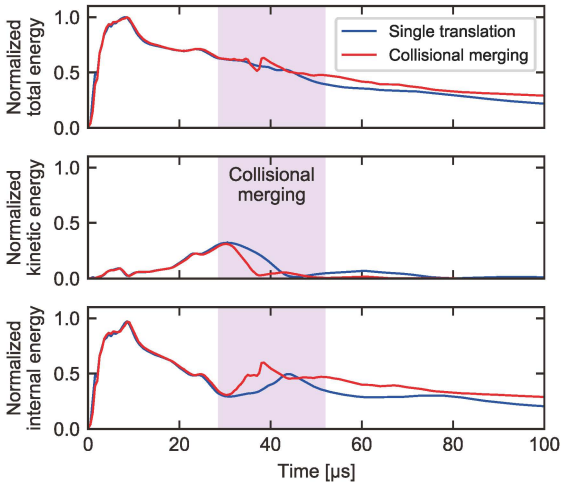

Fig. 4 Time evolution of normalized total, kinetic, and internal energy in the MHD simulation.

to compare with the collisional merging case. Figure 3 (b) shows a breakdown of energy before and after the collision. The energy of the two plasmoids just before the collision was estimated from the energy of the single translation case near the timing of the collision (t ~ 35 μs). Here the toroidal rotation energy of FRCs is neglected because it is several Joules, which is sufficiently smaller than any other energy. The plasmoids experience destructive disturbance in the collisional merging process. However, rather than the plasmoids being destructed in the collisional merging process, the energy decay is suppressed compared with the single translation case. This indicates that the kinetic energy regenerates back into internal thermal energy via a collisional merging process.

A similar energy flow trend was observed in a two-dimensional resistive magnetohydrodynamics (MHD) simulation. The simulation code, called Lamy Ridge, consists of resistive MHD equations and fluid equations [11, 12]. This code has been developed to simulate the collisional merging formation of FRCs. The MHD equations, supplemented with energy equations, exchange the density, momentum, and energy with fluid equations via ionization. A shockwave is modeled using the sharp and monotonic algorithm for realistic transport method, which is a modern shock-capturing method [13]. The plasma pressure and global motion of the FRC in the FAT-CM device have been successfully reproduced [14]. The time evolution of the simulated FRC energy is shown in Fig. 4. The energy is normalized by the maximum value of total energy in each case. In the collisional merging case, the kinetic energy efficiently regenerated back into the internal energy compared with the single plasmoid translation case, as was observed in the experiments. This simulation result supports the experimental observations. Therefore, it is suggested that the "collision of plasmoids" is an important process in the regeneration of kinetic energy.

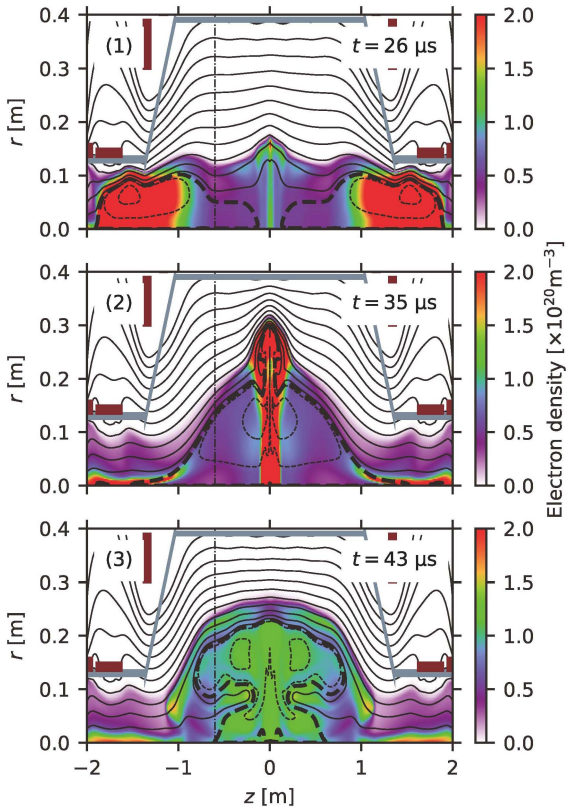

Fig. 5 Contour maps of computed electron density under the typical condition in the FAT-CM device. Solid lines and dashed lines denote the magnetic field line. The dashed bold line denotes the separatrix. The vertical dashed-dotted line denotes $z = -0.6$ m.

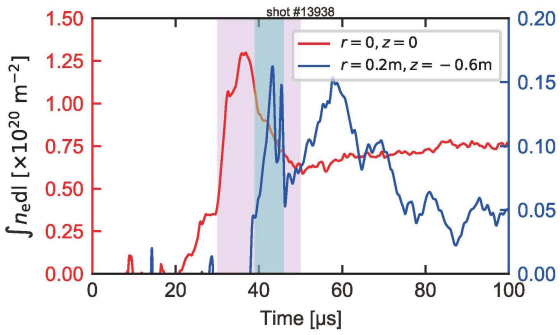

Fig. 6 Time evolution of the line-integrated electron density at mid-plane and cross-section of $r = 0.2$ m, $z = -0.6$ m.

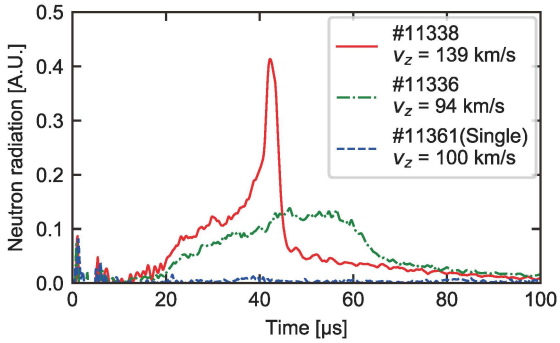

Fig. 7 Time evolution of neutron radiation.

4.2 Side evidence of shockwave excitation

Side evidence suggesting shockwave excitation was also observed. In the electron density measurements, a steep change in the electron density waveform was observed at two different sections. Figure 5 shows the line-integrated electron density at the mid-plane (red line) and the cross-section of $r = 0.2$ m and $z = -0.6$ m (blue line). The steep change in the blue line was delayed by that at mid-plane. This result suggests the formation and propagation of a shock front. A shock front was also observed in the MHD simulation. Figure 6 shows contour maps of the computed electron density. A high-density region suggesting a shock front was formed in the collision process ($t \sim 35$ μs).

The typical ion temperature was ~100 eV after collisional merging. The tail component of a Maxwell-Boltzmann distribution with the typical ion temperature of ~100 eV has sufficient energy to drive a deuterium-deuterium (D-D) reaction. However, the neutron generation rate calculated from the typical ion temperature (100 eV), electron density (10^{20} m^{-3}), and volume (0.2 m^3) of the merged FRC is too small (~10^{-6} neutrons per second) to be detected in the timescale of the collisional merging process (~20 μs). Therefore, a D-D reaction in thermal equilibrium plasma with the aforementioned ion temperature should not occur. In the experiments, neutron radiation was observed in collisional merging, as shown in Fig. 7. The red solid line and green dashed-dotted line in the figure denote the collisional merging cases and the blue dashed line denotes the single plasmoid translation case. This observation suggests ion acceleration and its dependency on the relative velocity at the collision. In previous work, related ramp up of soft X-ray radiation, which indicates plasma heating, has also been observed after collisional merging [15].

Comprehensively considering these results, it is expected that shockwaves are excited via collision of plasmoids at super Alfvénic/sonic speed and that the excited shock causes energy regeneration of kinetic energy back into thermal plasma energy.

5. Summary

The energy regeneration from kinetic energy back into internal thermal energy in the collisional merging process of FRCs was experimentally observed by simultaneous multi-pointed energy measurements in the FAT-CM device.

Shockwave excitation during the collisional merging process is suggested from density, neutron, and soft X-ray radiation observations. Particle acceleration should occur around shockwaves [16] and accelerated high-energy parti-

cles thermalize in the plasma. The shockwave may play an important role in the observed regeneration process, from kinetic to thermal energy.

Acknowledgments

The authors would like to acknowledge Dr. Sean Dettrick, Dr. Yung Mok, and all members of the Fusion-Plasma group, Nihon University. This work was partially supported by JSPS KAKENHI Grant Number JP20H00143, JP19K21868, JP16K06939, Nihon University, College of Science and Technology, Grant for Project Research, and Nihon University, College of Science and Technology, Grants-in-Aid.

[1] M. Tuszewski, Nucl. Fusion **28**, 2033 (1988).
[2] L.C. Steinhauer, Phys. Plasmas **18**, 070501 (2011).
[3] T. Asai, Ts. Takahashi, J. Sekiguchi, D. Kobayashi, S. Okada *et al.*, Nucl. Fusion **59**, 056024 (2019).
[4] H. Guo, M. Binderbauer, D. Barnes, S. Putvinski, N. Rostoker *et al.*, Phys. Plasmas **18**, 056110 (2011).
[5] H. Gota, M.W. Binderbauer, T. Tajima, S. Putvinski, M. Tuszewski *et al.*, Nucl. Fusion **59**, 112009 (2019).
[6] H. Himura, S. Okada, S. Sugimoto and S. Goto, Phys. Plasmas **2**, 191 (1995).
[7] H. Himura, S. Ueoka, M. Hase, R. Yoshida, S. Okada and S. Goto, Phys. Plasmas **5**, 4262 (1998).
[8] M.W. Binderbauer, H.Y. Guo, M. Tuszewski, S. Putvinski, L. Sevier *et al.*, Phys. Rev. Lett. **105**, 045003 (2010).
[9] D.J. Rej, W.T. Armstrong, R.E. Chrien, P.L. Klingner and R.K. Linford *et al.*, Phys. Fluids **29**, 852 (1986).
[10] L.C. Steinhauer, H. Guo, A. Hoffman, A. Ishida and D. Ryutov, Phys. Plasmas **13**, 056119 (2006).
[11] Y. Mok, D. Barnes and S. Dettrick, Bull. Am. Phys. Soc. **55**, GP9.97 (2010).
[12] M. Onofri, P. Yushmanov, S. Dettrick, D. Barnes, K. Hubbard and T. Tajima, Phys. Plasmas **24**, 092518 (2017).
[13] P.H. Gaskell and A.K.C. Lau, Int. J. Numer. Methods Fluids **8**, 617 (1988).
[14] D. Kobayashi, T. Asai, Ts. Takahashi, J. Sekiguchi, H. Gota, S. Dettrick, Y. Mok, M. Binderbauer and T. Tajima, Plasma Fusion Res. **15**, 2402020 (2020).
[15] J. Sekiguchi, T. Asai and Ts. Takahashi, Plasma Fusion Res. **14**, 3402116 (2019).
[16] R. Blandford and D. Eichler, Phys. Rep. **154**, 1 (1987).